Indonesian Journal of Electrical Engineering and Computer Science
Vol. 41, No. 1, January 2026, pp. 3∼17
ISSN: 2502-4752, DOI: 10.11591/ijeecs.v41.i1.pp3-17

Dynamic behavior of induction machines in ATP-EMTP with space harmonics

Jose Manuel Aller, Ruben Nicolas Guevara, Bryam Steven Pulla
Department of Electrical Energy, Universidad Politecnica Salesiana (UPS), Cuenca, Ecuador

Article Info

Article history:

Received Apr 4, 2025
Revised Dec 5, 2025
Accepted Dec 14, 2025

Keywords:

ATP-EMTP
Induction machine
Space harmonics
Transient analysis
VBR model

ABSTRACT

This work develops a space-vector model of a squirrel-cage induction machine that incorporates the effects of spatial harmonics arising from the winding distribution. The modeling approach includes the first, fifth, and seventh spatial harmonics, which are the components with the greatest influence on the machine's magnetic field. Simulation results highlight the impact of these harmonics on the stator and rotor currents, the electromagnetic torque, and the machine's speed. To build the model, the voltage behind reactances (VBR) technique is employed, enabling a hybrid strategy that combines circuit-based modeling tools—such as ATP-EMTP—with computational programming in models to complement the solution of the differential equations governing the behavior of the electromechanical system. This methodology effectively transforms the induction machine into a dynamic Thèvenin-equivalent circuit for each phase of the converter. This study provides a useful framework for evaluating how space harmonics affect the performance and operating characteristics of induction machines. The models were implemented using the ATP-EMTP software and its graphical interface, ATPDraw.

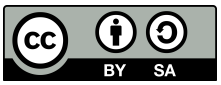

Corresponding Author:

Jose Manuel Aller
Department of Electrical Energy, Universidad Politecnica Salesiana (UPS)
Sede Cuenca, Calle Vieja y Elia Liut, 010105 Cuenca, Ecuador
Email: jaller@ups.edu.ec

1. INTRODUCTION

The induction machine is currently the most widely used electromechanical converter. Its robustness, reliability, and low maintenance requirements enable it to operate even under very harsh conditions [1], [2]. Its invention is attributed to Nicola Tesla, who developed the concept of the rotating magnetic field in 1888 [3]. However, during the same period, the Italian Galilera Ferraris presented similar work between 1885 and 1888 [4], [5]. Later, in Dolivo-Dobrovolsky [6] and Ferraris and Arno [7] introduced the use of three-phase coils in the induction machine, which is now standard in electrical distribution systems. This development laid the foundation for modern electrical industry, providing significant performance, versatility, and reliability across various sectors [8].

The space harmonics generated by the space distribution of the stator and rotor windings affect the machine's performance, which has been extensively studied [9], [10]. These harmonics alter the distribution of the magnetic field and can generate fluctuations in electrical torque, distorted voltage waveforms, losses and noise that affect the efficiency and operational characteristics of the machine [11]–[13].

This article models the induction machine, considering the first, fifth, and seventh space harmonics, which are the most important components of the field in the air gap. This type of model allows for the devel-

opment of speed measurement strategies using the harmonic spectrum of the currents [14], [15]. The approach used consists of representing the machine through space vectors where both the stator and rotor refer to their respective reference systems [16], [17], due to the presence of space harmonics that prevent simplifying the dependence on the angular position θ of the rotor when transforming the equations to the stator reference.

The voltage behind reactance (VBR) model is a widely used method for representing induction machines due to its improved numerical efficiency and flexibility compared to traditional models [18], [19]. In the modeling, the VBR approach is applied, which facilitates analysis by representing the internal voltage of the machine as a combination of electromotive force, resistance, and inductance whose parameters vary over time with the rotor's position. This approach has been utilized by several authors for the integration of the machine with its electronic drives, but the inclusion of space harmonics in this type of modeling is unprecedented, even though [20] has proposed an approach based on the VBR technique to include the effects of saturation in the induction machine.

Furthermore, this model is implemented using the ATP-EMTP tool and its graphical environment ATPDraw [21], [22] to study the impact of space harmonics on key variables such as angular speed, electrical torque, and currents. This approach allows for obtaining a more accurate model of the induction machine, which facilitates the evaluation of losses, efficiency, and its operational characteristics [23]–[25].

2. METHOD

2.1. Statement of the theoretical problem

The analysis of the dynamic behavior of induction machines is fundamental to ensuring the stability and efficiency of modern electrical systems [26], [27]. These machines represent an essential component in industrial, commercial, and power generation applications, where their proper modeling allows for predicting their response under different operating conditions. However, the presence of space harmonics in their operation introduces complex phenomena that affect their performance, generating current distortions, variations in electromagnetic torque, and additional losses in the system [11]-[13].

Space harmonics are produced by the geometry of the air gap, the winding distribution, and magnetic saturation, generating adverse effects on the operation of induction machines. Consequently, the precise simulation of these effects is crucial for evaluating their impact on the stability of the electrical system and the efficiency of devices connected to the grid [20].

In this context, there is a need to develop a model that realistically represents the dynamic behavior of induction machines, considering the effects of space harmonics and validating it through simulations in ATP-EMTP. This study aims to bridge the existing gap between theory and practice by implementing more accurate models. The validation of these models will improve the design of induction machines by implementing new technologies to filter the harmonics produced by the induction machine. Furthermore, this model will allow for observing the impact of these harmonics on electrical parameters such as torque, angular speed, currents in the stator, among others. In this way, it will contribute to mitigating these effects and aid in the constructability of the machine.

2.2. VBR model of the IM considering first harmonic space distribution

The voltage equations of the IM in space vectors can be represented as [28]:

$$\begin{bmatrix} \vec{v_s} \\ 0 \end{bmatrix} = \begin{bmatrix} R_s & 0 \\ 0 & R_r \end{bmatrix} \begin{bmatrix} \vec{i_s} \\ \vec{i_r} \end{bmatrix} + p \begin{bmatrix} \vec{\lambda_s} \\ \vec{\lambda_r} \end{bmatrix} \tag{1}$$

where,

$$\begin{bmatrix} \vec{\lambda_s} \\ \vec{\lambda_r} \end{bmatrix} = \begin{bmatrix} L_s & M_1 e^{j\theta} \\ M_1 e^{-j\theta} & L_r \end{bmatrix} \begin{bmatrix} \vec{i_s} \\ \vec{i_r} \end{bmatrix} \tag{2}$$

From (1) and (2), we obtain,

$$p\vec{\lambda_r} = -\frac{R_r}{L_r}\left(\vec{\lambda_r} - M_1 e^{-j\theta}\vec{i_s}\right) \tag{3}$$

and,

$$\vec{ir} = \frac{1}{Lr}\left(\vec{\lambda_r} - M_1 e^{-j\theta}\vec{i}_s\right) \tag{4}$$

Introducing (3) and (4) into the stator voltage equation $\vec{v_s}$ (1), we obtain the VBR model, which is a dynamic Thèvenin equivalent:

$$\vec{v_s} = R_{eq}, \vec{i_s} + L_{eq}, p\vec{i_{eq}} + \vec{e}_{eq}, \tag{5}$$

where:

$$R_{eq} = \left(R_s + R_r \frac{M_1^2}{L_r^2}\right) \tag{6}$$

$$L_{eq} = \left(L_s - \frac{M_1^2}{L_r}\right) \tag{7}$$

$$\vec{e}_{eq} = \frac{M1}{L_r}\left(j\dot{\theta} - \frac{R_r}{L_r}\right) e^{j\theta}\vec{\lambda}_r \tag{8}$$

The electrical torque in space vectors is obtained from,

$$T_{e1} = M_1 \Im m\left\{\vec{i}_s \left(\vec{i}_r e^{j\theta}\right)^*\right\} = \frac{M_1}{L_r}\Im m\left\{\vec{i}_s \left(\vec{\lambda}_r e^{j\theta}\right)^*\right\} \tag{9}$$

In Figure 1, the VBR model of the IM in space vectors is presented, referenced to the stator and rotor axes, considering that the space distribution is of the first harmonic.

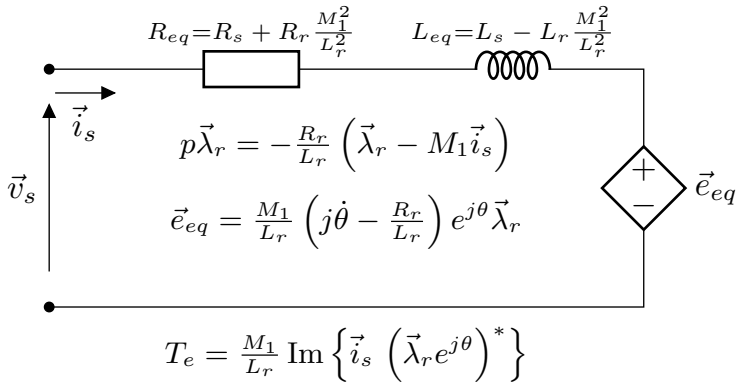

Figure 1. VBR model of the IM corresponding to the first space harmonic in stator-rotor coordinates

2.3. VBR model of the IM considering higher space harmonics

To assess the effect of space harmonics in the IM model, the contents of the first, fifth, and seventh space harmonics are included, as they have the most significant magnitudes. However, the proposed method can be generalized to any number of harmonics in space. The third harmonic in balanced three-phase machines is generally negligible and, for this reason, it has not been considered in this model.

The (1) is valid for any number of harmonics. The fundamental difference lies in the determination of the inductance matrix and its relationship with the flux links:

$$\begin{bmatrix} \vec{\lambda}_s \\ \vec{\lambda}_r \end{bmatrix} = \begin{bmatrix} L_s & \sum M_{sr_i}(\theta) \\ \sum M^*_{rs_i}(\theta) & L_r \end{bmatrix} \begin{bmatrix} \vec{i}_s \\ \vec{i}_r \end{bmatrix} \tag{10}$$

where:

$$\sum M_{sr_i}(\theta) = M_1 e^{j\theta} + M_5 e^{-j5\theta} + M_7 e^{j7\theta} + M_{11} e^{-j11\theta} + M_{13} e^{j13\theta} + \cdots$$

From expression (10), we obtain:

$$\vec{ir} = \frac{1}{Lr}\left(\vec{\lambda}r - \sum M^*_{rs_i}(\theta)\ \vec{i}_s\right) \tag{11}$$

and replacing (11) in (1), we have:

$$p\vec{\lambda}_r = -\frac{R_r}{L_r}\left(\vec{\lambda}_r - \sum M^*_{rs_i}(\theta)\ \vec{i}_s\right) \tag{12}$$

The stator voltage equation, obtained from (1), including the effect of the space harmonics, is:

$$\vec{v}_s = R_s\vec{i}_s + p\left(L_s\vec{i}_s + \sum M_{sr_i}(\theta)\ \vec{i}_r\right) \tag{13}$$

By substituting (11) and (12) into (13), we obtain:

$$R_{eq} = R_s + \frac{R_r}{L_r^2}\left\{M_1^2 + M_5^2 + M_7^2 + .\cdots + 2\left(M_1M_5 + M_1M_7 + M_5M_7\right)\cos 6\theta + \cdots\right\} \tag{14}$$

The equivalent inductance L_{eq} is:

$$L_{eq} = L_s - \frac{1}{L_r}\left\{M_1^2 + M_5^2 + M_7^2 + .\cdots + 2\left(M_1M_5 + M_1M_7 + M_5M_7\right)\cos 6\theta + .\cdots\right\} \tag{15}$$

The electromotive force $\vec{e}_e$ is:

$$\vec{e}_{eq} = \left[-\frac{R_r}{L_r}A + j\dot{\theta}\frac{\partial A}{\partial\theta}\right]\frac{\vec{\lambda}_r}{L_r} + 12\dot{\theta}\frac{B}{L_r}\sin 6\theta\,\vec{i}_s \tag{16}$$

where:

$$A = \left(M_1 e^{j\theta} + M_5 e^{-j5\theta} + M_7 e^{j7\theta}\right)$$

$$B = M_1M_5 + M_1M_7 + 4M_5M_7\cos 6\theta$$

Finally, the electrical torque can be determined as:

$$T_e = T_{e_1} + T_{e_5} + T_{e_7} \tag{17}$$

where,

$$T_{e_1} = \frac{M_1}{L_r}\Im m\left\{\vec{i}_s\ \left(\vec{\lambda}_r e^{j\theta}\right)^*\right\} \tag{18}$$

$$T_{e_5} = -\frac{5M_5}{L_r}\Im m\left\{\vec{i}_s\ \left(\vec{\lambda}_r e^{j5\theta}\right)^*\right\} \tag{19}$$

$$T_{e_7} = \frac{7M_7}{L_r}\Im m\left\{\vec{i}_s\ \left(\vec{\lambda}_r e^{j7\theta}\right)^*\right\} \tag{20}$$

The VBR model is a dynamic equivalent of the differential equations of the machine that allows it to be represented by an electrical circuit with R_{eq}, L_{eq}, and an electromotive force $\vec{e}_{eq}$. The variables used are space vectors obtained from the general expression:

$$\vec{x}_s = \sqrt{\frac{2}{3}}\left\{x_a(t) + e^{j\frac{2\pi}{3}}x_b(t) + e^{j\frac{4\pi}{3}}x_c(t)\right\} \tag{21}$$

The equivalent resistance R_{eq} and inductance L_{eq} can be directly used in each of the phases of an electrical circuit. The rotor's flux link can be obtained by numerically integrating the differential (3). With this information, it is possible to determine the space vector of the electromotive force $\vec{e_{eq}}$. To determine the electromotive forces of each phase of the IM, the inverse transformations are used:

$$x_a(t) = \sqrt{\frac{2}{3}} \Re e \{\vec{x}_s\} \tag{22}$$

$$x_b(t) = \sqrt{\frac{2}{3}} \Re e \left\{\vec{x}_s e^{j\frac{4\pi}{3}}\right\} \tag{23}$$

$$x_a(t) = \sqrt{\frac{2}{3}} \Re e \left\{\vec{x}_s e^{j\frac{2\pi}{3}}\right\} \tag{24}$$

2.4. VBR model of the IM in ATPDraw

Figure 2 represents the dynamic model of an induction machine developed in the graphical environment of ATPDraw from the ATP-EMTP program, including the influence of space harmonics. The model includes the three phases of the IM, calculating within the simulation models block the rotor's flux link, which allows for the determination of instantaneous values of R_{eq}, L_{eq} , e_a, e_b y e_c. The dependent electromotive forces must be simulated using Norton equivalents because the tool does not have isolated dependent voltage sources from ground.

One of the main difficulties with programming in models is that it requires separating the variables into real and imaginary parts, as this tool does not handle complex numbers. The programming used to create the model can be found in section 4.2.1, where the variables denoted with x represent the real part and those with y represent the imaginary part of the space vector.

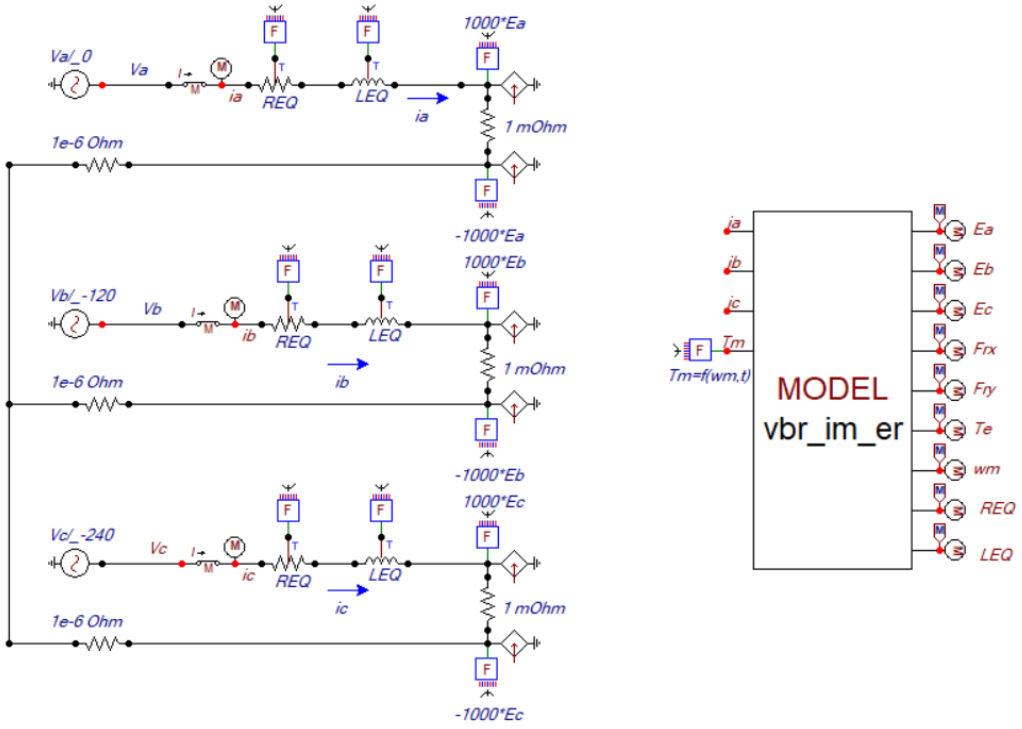

Figure 2. Model in ATPDraw of a VBR induction machine for space harmonic analysis

3. RESULTS

3.1. Results of the VBR model of the IM

In Table 1, the data used to analyze the behavior of the IM is presented.

Table 1. Data of the IM used in the VBR modeling

Parameter	Value
R_s	$0.353\,\Omega$
R_r	$0.424\,\Omega$
L_{ls}	$2.59\,mH$
L_{lr}	$3.88\,mH$
p	$2\,pair$
M_{sr1}	$67.47\,mH$
M_{sr5}	$0.60\,mH$
M_{sr7}	$0.60\,mH$
J	$0.163\,kg\,m^2$
k_r	$0.002\,W/(rad/s)^2$

3.1.1. Results corresponding to the simulation with fundamental harmonic in space

In Figure 3, the results obtained with the VBR model of the IM are shown, considering the behavior of the first, fifth, and seventh space harmonics. In Figure 4, the behavior of the currents obtained is represented for the same case, considering in the simulation only the first space harmonic. Figure 5 presents a detail of the machine's currents in steady state when only the first harmonic is considered in the space distribution. In this case, the stator currents also exhibit a first temporal harmonic.

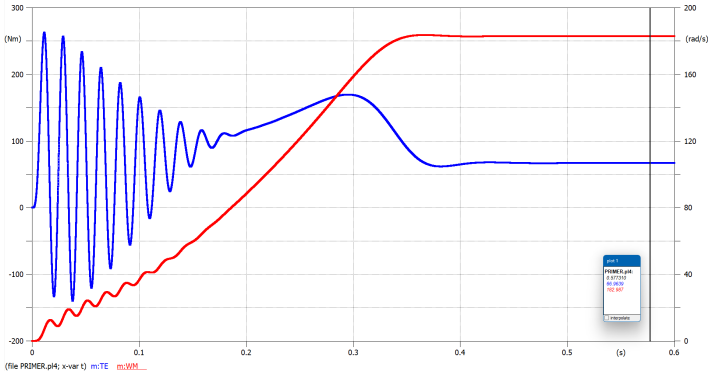

Figure 3. Electrical torque and angular speed of the IM considering the fundamental harmonic

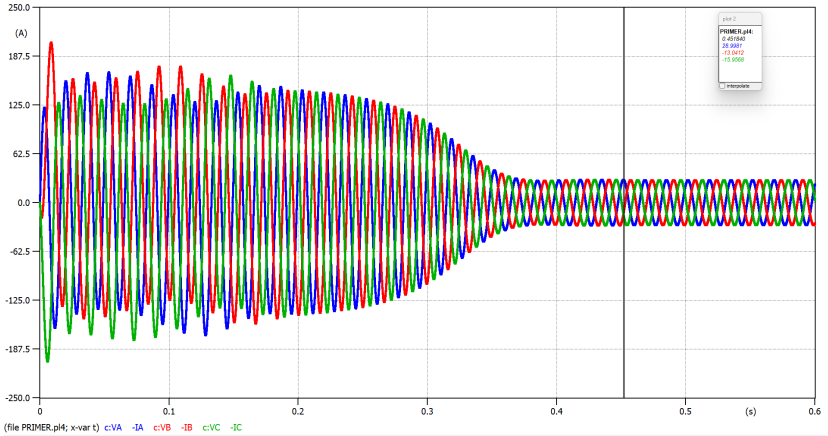

Figure 4. Currents in phases a, b, and c of the IM stator, considering the fundamental harmonic

Figure 6 shows the Fourier spectrum of the currents obtained in the simulation, where it is observed that only the presence of the first temporal harmonic exists due to the space distribution, which includes only the fundamental component. Finally, Figure 7 presents the development of the space vectors of the rotor flux of the IM during startup.

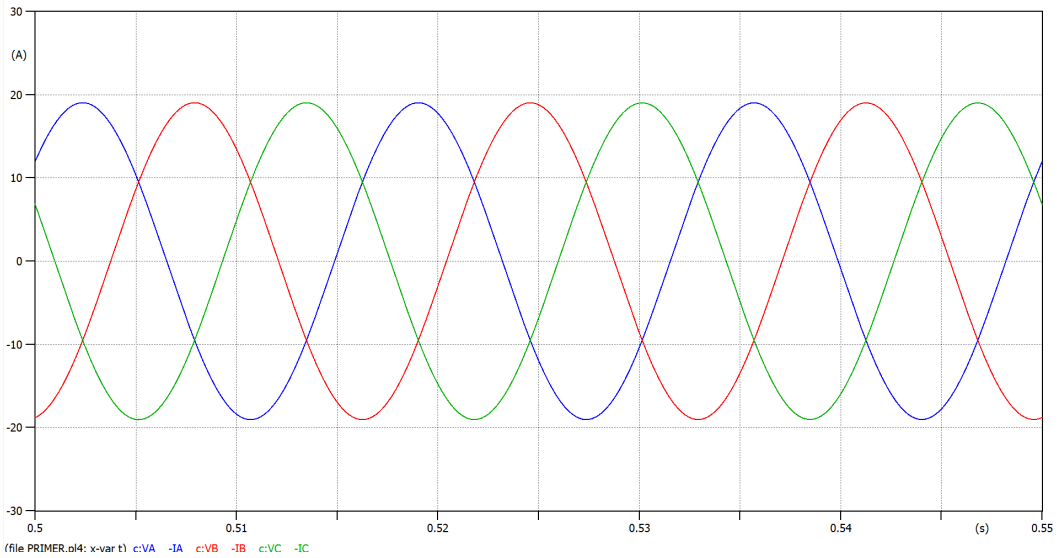

Figure 5. Currents in phases a, b, and c of the IM stator, considering the fundamental harmonic

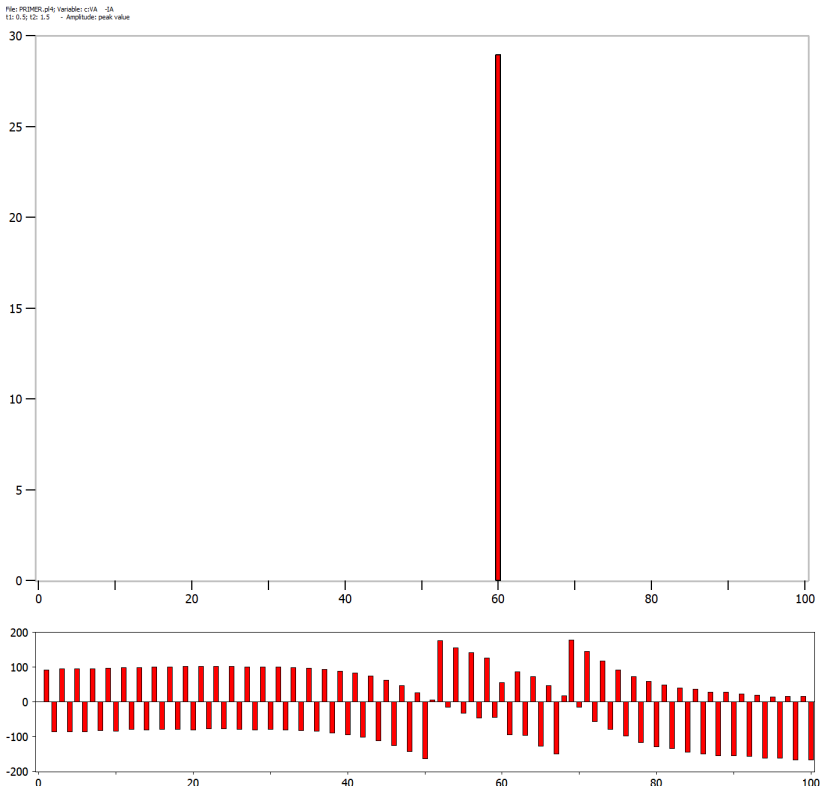

Figure 6. Fourier spectrum of the currents obtained in the VBR simulation of the IM with first harmonic space distribution

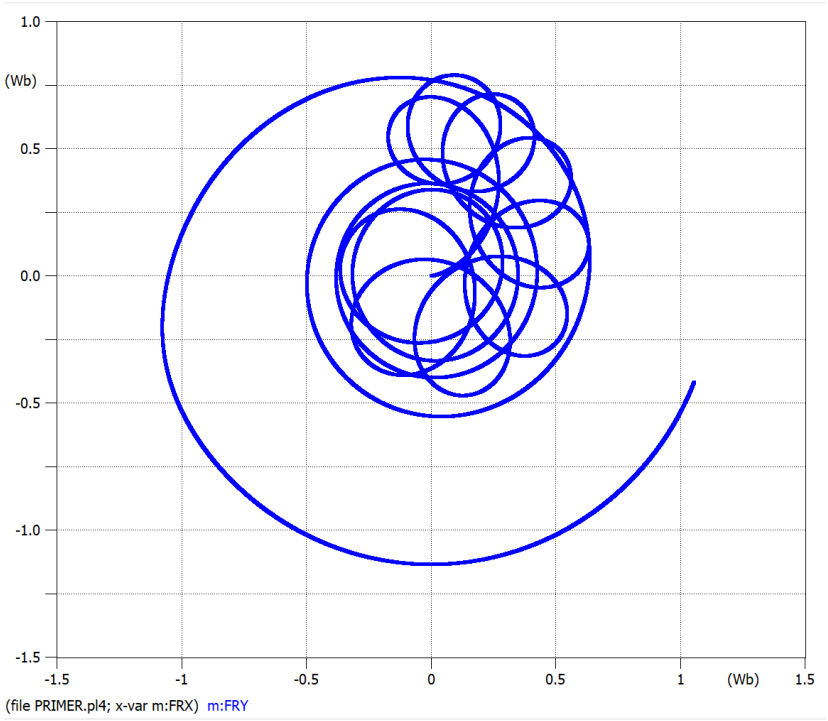

Figure 7. Evolution of the space vector of the rotor flux linkages $\vec{\lambda_r}$ during the startup of the IM

3.1.2. Results corresponding to the simulation considering first, fifth, and seventh space harmonics

In Figure 8, the results obtained with the VBR model of the IM are shown, considering the behavior of the first three space harmonics. In Figure 9, the behavior of the currents obtained is represented for the same case, considering the simulation of the first three space harmonics. Figure 10 shows a detail of the steady-state currents where the presence of temporal harmonics caused by the space harmonic distribution in the air gap is observed.

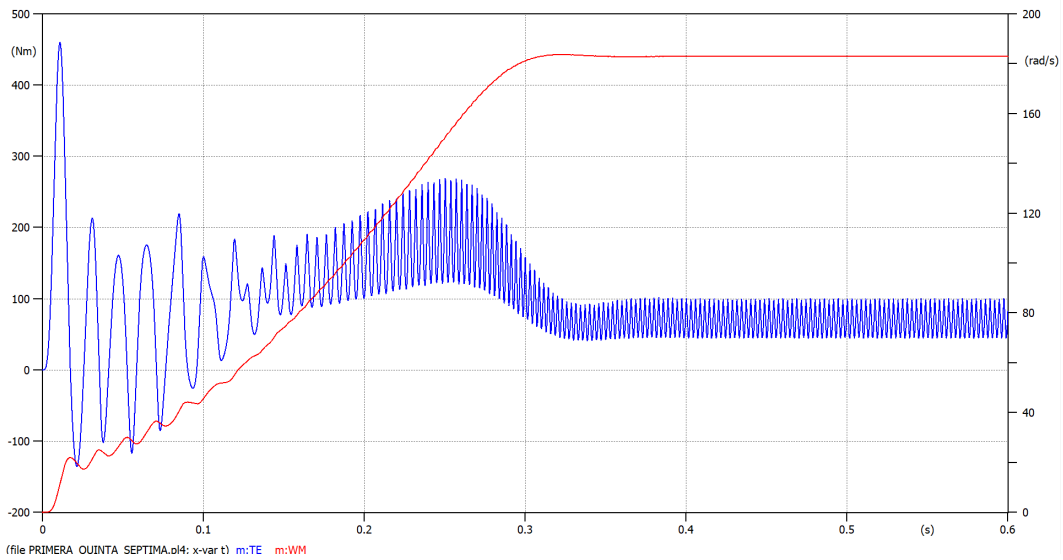

Figure 8. Electrical torque and angular speed of the IM considering the first, fifth, and seventh space harmonics

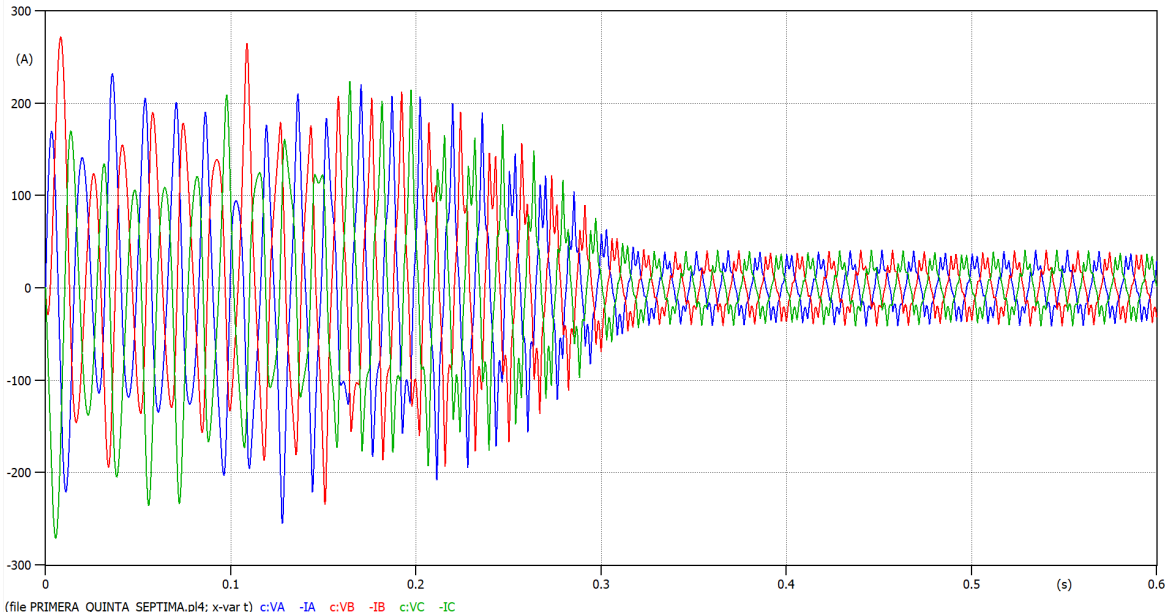

Figure 9. Currents in phases a, b, and c of the IM stator, considering the first, fifth, and seventh harmonics

Figure 11 presents the Fourier spectrum of the currents obtained in the simulation, where the presence of the first, fifth, and seventh temporal harmonics in the currents can be observed, along with their multiples, due to the space distribution that includes the first, fifth, and seventh space harmonics. Finally, Figure 12 presents the development of the space vectors of the rotor flux of the IM during startup, considering the first three space harmonics.

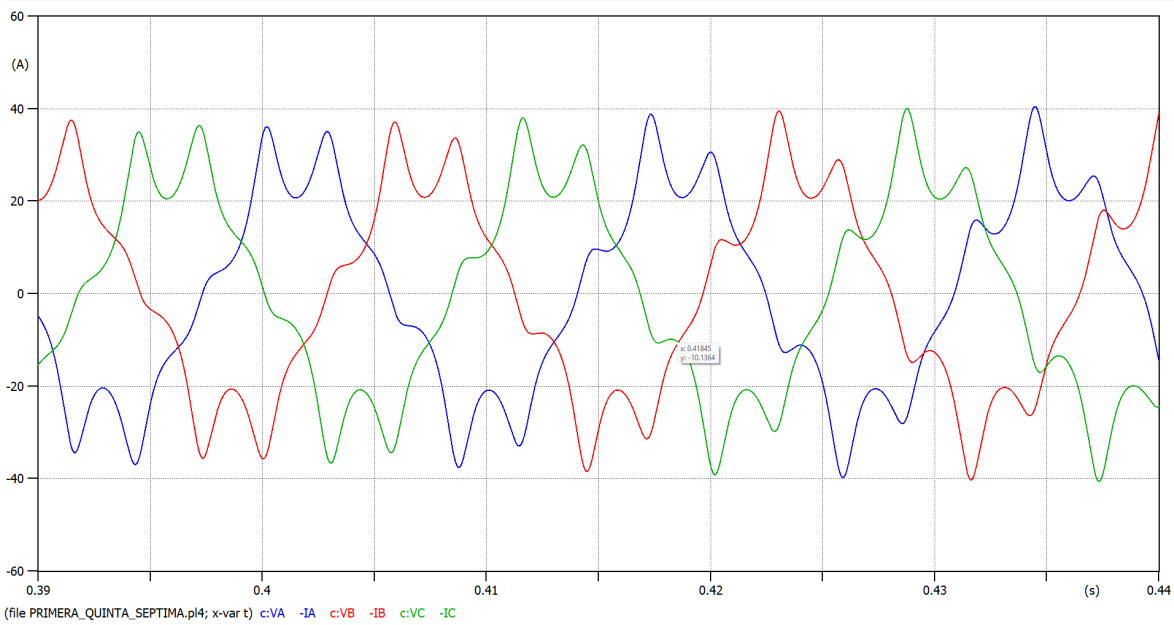

Figure 10. Detail of the steady-state currents in phases a, b, and c of the IM stator, considering the first, fifth, and seventh harmonics

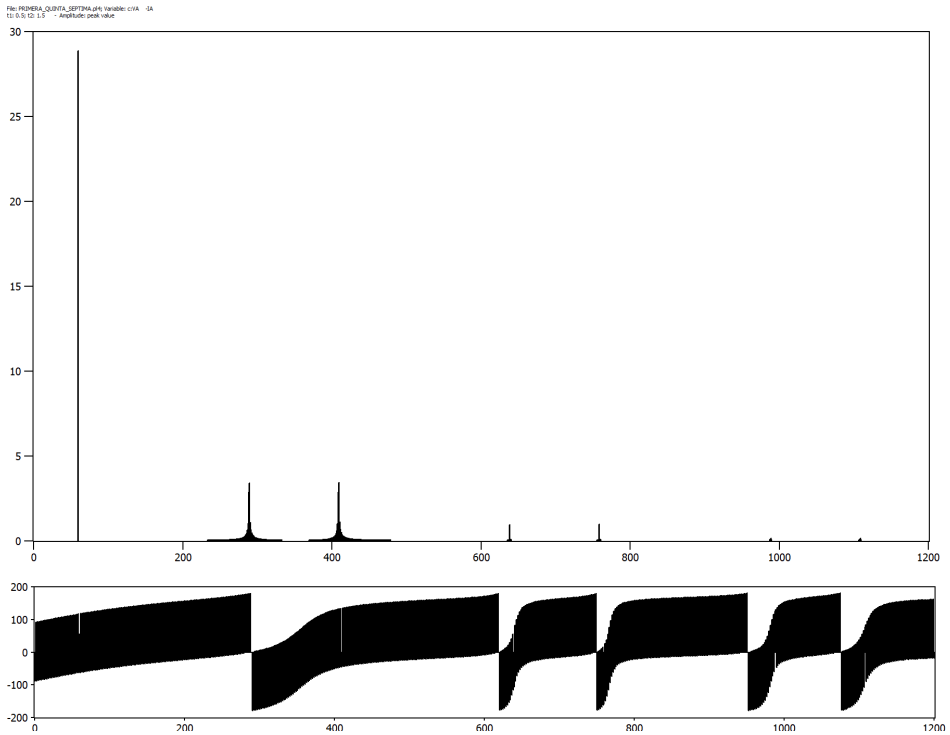

Figure 11. Fourier spectrum of the currents obtained in the VBR simulation of the IM with space distribution of the first, fifth, and seventh space harmonics

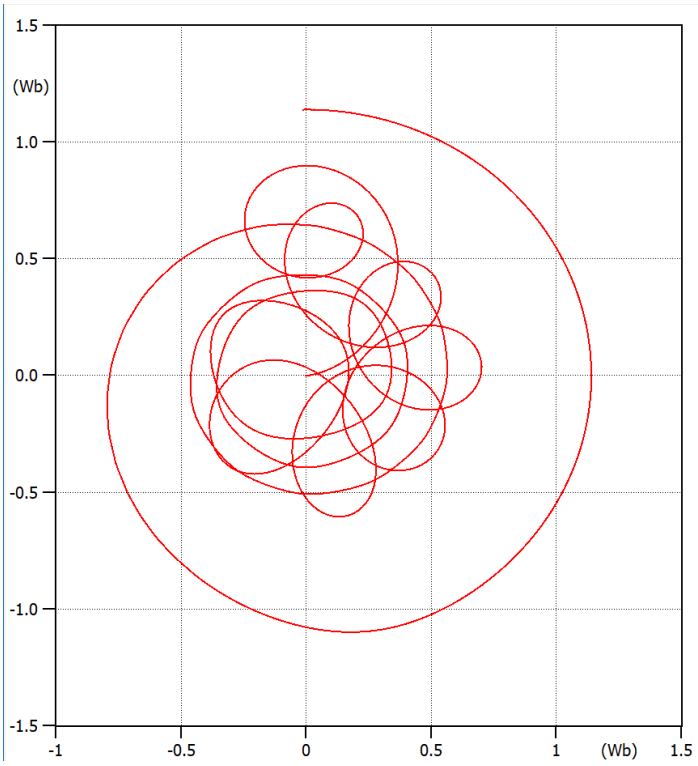

Figure 12. Evolution of the space vector of the rotor flux linkages $\vec{\lambda}_r$ during the startup of the IM considering the first three space harmonics

4. DISCUSSION

4.1. Result analysis for first harmonic

The results obtained reveal that modeling the induction machine using the VBR technique provides a simple and accurate representation of the fundamental harmonic in space. The model obtained in stator and rotor coordinates aligns with the models referred to the stator. As can be seen in Figure 3, where the electrical torque and speed are represented for an induction machine that has a space distribution of the first harmonic field that matches the results obtained in the models presented in [28]. In Figures 4, 6, and 7, the stator currents, the spectrum of these currents, and the space vector of the rotor flux linkage are represented under the same condition, respectively.

4.2. Result analysis for first, fifth and seventh harmonic

To consider the effect of space harmonics, it is necessary to apply the principle of superposition, summing the different harmonics in the mutual inductances and in the calculation of the electrical torque. As the harmonic number increases, its amplitude and influence on the various electrical variables decrease. A particular case is the rotor flux linkage where space harmonics have a very limited influence, unlike the electrical torque where these harmonics produce significant fluctuations that manifest as reduced stability in the machine's velocity. Some harmonics rotate in the opposite direction to the machine's speed, introducing larger losses in the converter. Each harmonic generates an associated electrical torque, so the total torque is obtained by summing the individual torques of each harmonic. The harmonic electrical torque tends to progressively decrease in magnitude, although its effect is noticeable in the lower harmonics.

In Figure 8, the behavior of the speed ω_m and the electrical torque T_e is shown when the first, fifth, and seventh space harmonics are included in the representation of the inductances of the induction machine. The stator currents, their spectrum, and the space vector of the rotor flux linkage are presented in Figures 9, 11, and 12, respectively. In these results, the influence of the space harmonics on torque and angular speed can be clearly detected. In the rotor flux linkages, the influence is less decisive.

4.2.1. ATPdraw circuit model

Figure 13 shows the ATP-EMTP implementation of the induction machine model considering first, fifth, and seventh space harmonics in the air gap. The Figure 14, presents the complete and commented code in models language for ATP-EMTP. Models code for the induction machine model considering harmonics first, fifth and seventh [29]. This code reads the input parameters of the machine being simulated, assigning default values in case they are not defined in the call. It also defines the input variables from the VBR circuit, which are read, as well as the output variables that are sent to the circuit or to the results output. State variables are defined in the history to enable subsequent integrations of the differential equations. The next step involves assigning initial values to these variables.

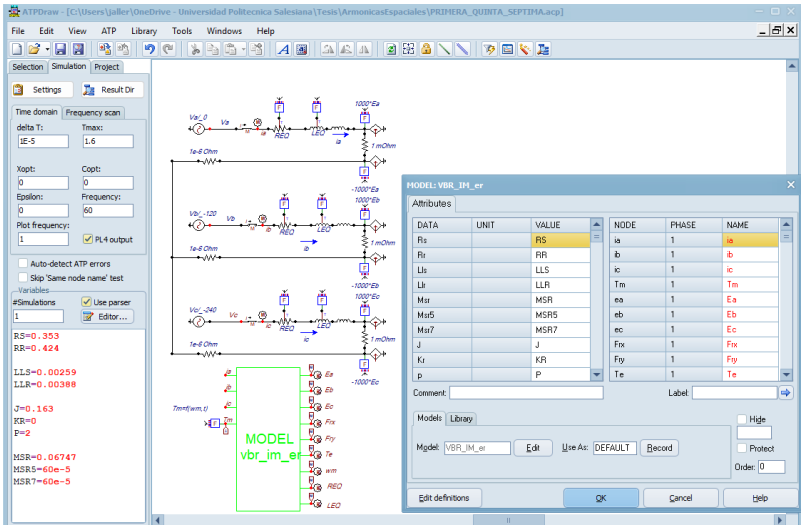

Figure 13. ATPDraw model for induction motor considering space harmonics

```
MODEL VBR_IM_er -- HArmonic induction motor model
DATA Rs (dflt: 0.353),Rr (dflt: 0.428) -- Default parameters
DATA Lls (dflt: 2.59e-3),Llr (dflt: 3.88e-3),Mar (dflt: 67.47e-3),Mar5 (dflt: 60.e-5);
DATA Mar7 (dflt: 60.e-7), J (dflt: 0.163),Kr (dflt:0),p (dflt:2)
INPUT ia, ib, ic, Tm -- input variables from circuit
CONST SQRT23 (val: 0.816496581),SQRT1_2 (val: 0.707106781)
CONST SQRT1_6 (val: 0.408248290),SQRT1_3 (val: 0.577350269)
OUTPUT oa,ob,oc,Frx,Fry,Te,wm,REQ,LEQ --output variables
VAR oa,ob,oc,Frx,Fry,Te,wm,ix,iy,io,pFrx,pFry,REQ,LEQ
VAR ox,oy,oo,pwm,Lr,Ls,M1,M5,M7,TETITA,THETA,To5,To7,ox5,ox7,oy5,oy7
VAR AUX1,AUX2,AUX3,AUX4,AUX5,AUX6,AUX7,AUX8,AUX9,AUX10,AUX11,AUX12
VAR AUX13,AUX14,AUX15,AUX16,AUX17,AUX18,AUX20
HISTORY -- Storing previous values for integration variables
  pFrx (dflt:0)                    -- Fluxes derivatives
  integral(pFrx) (dflt:0)
  pFry (dflt:0)
  integral(pFry) (dflt:0)
  pwm (dflt:0)                     -- Angular speed derivative
  integral(pwm) (dflt:0)
  io (dflt:0)                      -- cero sequence current
  wm (dflt:0)
  integral(wm)(dflt:0)
INIT
ENDINIT
EXEC
  Lr:=(Llr+Mar) -- Rotor inductance
  Ls:=(Lls+M3R)
  M1 := Mar -- Mutual inductance
  M5 := Mar5
  M7 := Mar7
   -- Transformation from stator currents to space vector components ix, iy, io
  ix:= SQRT23*(ia-0.5*ib-0.5*ic)
  iy:= SQRT1_2*(ib-ic)
  io:= SQRT1_2*(ia+ib+ic)
  -- Auxiliar variables
  AUX1:=Frx*cos(totita)-Fry*sin(totita)
  AUX2:=Frx*sin(totita)+Fry*cos(totita)
  AUX3:=ix*cos(totita)+iy*sin(totita)
  AUX4:=iy*cos(totita)-ix*sin(totita)
  AUX5:=Frx*cos(5*totita)+Fry*sin(5*totita)
  AUX6:=Frx*sin(5*totita)-Fry*cos(5*totita)
  AUX7:=ix*cos(5*totita)-iy*sin(5*totita)
  AUX8:=iy*cos(5*totita)+ix*sin(5*totita)
  AUX9:=Frx*sin(5*totita)+Fry*cos(5*totita)
  AUX10:=Frx*cos(5*totita)-Fry*sin(5*totita)
  AUX11:=12*p*wm*(M1*M5/Lr)*sin(6*totita)
  AUX12:=12*p*wm*(M1*M7/Lr)*sin(6*totita)
  AUX13:=24*p*wm*(M5*M7/Lr)*sin(12*totita)
  AUX14:=Frx*cos(7*totita)-Fry*sin(7*totita)
  AUX15:=Frx*sin(7*totita)+Fry*cos(7*totita)
  AUX16:=ix*cos(7*totita)+iy*sin(7*totita)
  AUX17:=iy*cos(7*totita)-ix*sin(7*totita)
  AUX18:=2*M1*M7*cos(6*totita)+2*M5*M7*cos(6*totita)
  -- Rotor fluxes derivatives
  pFrx:=-Rr*(Frx-M1*AUX3-M5*AUX7-M7*AUX16)/Lr
  pFry:=-Rr*(Fry-M1*AUX4-M5*AUX8-M7*AUX17)/Lr
  -- Rotor fluxes integration
  Frx:=INTEGRAL(pFrx)
  Fry:=INTEGRAL(pFry)
 -- Req calculation
  REQ:=RS+(RR/(Lr**2))*M1**2+M5**2+M7**2+2*M1*M5*cos(6*totita)+AUX18
  -- Leq calculation
  LEQ:=(LE-(1/LR)*(M1**2+M5**2+M7**2+2*M1*M5*cos(6*totita)+AUX18))
  -- Eeq calculation in space vector coordinates
  ox7:=(M7*(-Rr*AUX14/Lr-p*wm*7*AUX15)/Lr)+(AUX11+AUX12+AUX13)*ix
  ox5:=(M5*(-Rr*AUX5/Lr-p*wm*5*AUX6)/Lr)
  ox:=(M1*(-Rr*AUX1/Lr-p*wm*AUX2)/Lr)+ox5+ox7
  oy7:=(M7*(p*wm*7*AUX14-Rr*AUX15/Lr)/Lr)+(AUX11+AUX12+AUX13)*iy
  oy5:=(M5*(-p*wm*5*AUX5+Rr*AUX6/Lr)/Lr)
  oy:=(M1*(p*wm*AUX1-Rr*AUX2/Lr)/Lr)+oy5+oy7
  oo:= Rs*io+lls*deriv(io)
  -- Eeq space vector transformation to abc
  oa:= SQRT23*ox+SQRT1_3*oo
  ob:=-SQRT1_6*ox+SQRT1_2*oy+SQRT1_3*oo
  oc:=-SQRT1_6*ox-SQRT1_2*oy+SQRT1_3*oo
  -- Electric torque calculation
  To5:=p*M5*(AUX9*ix-AUX10*iy-M5*sin(10*totita)*ix**2+M5*cos(10*totita)*iy**2)/Lr
  To7:=p*M7*(AUX14*iy-AUX15*ix)/Lr
  Te:=p*M1*(AUX1*iy-AUX2*ix)/Lr+To5+To7
  -- Dynamic equation -- angular speed derivative
  pwm:=(Te-Tm-Kr*wm)/J
    -- Integration of the dynamic equation
  wm:=INTEGRAL(pwm)  -- angular speed
  -- Integration
  Theta:=INTEGRAL(wm)
  totita:=p*Theta -- Mechanical angle
ENDEXEC
ENDMODEL
```

Figure 14. Models script for induction motor model considering space harmonics

Finally, the executable part begins, which occurs at each integration step, where the input variables are transformed into the space vector domain, the derivatives of the state variables are calculated, integrated, and ultimately converted back to the natural variable domain a, b, and c. Additionally, the angular velocity is calculated by integrating Newton's equation, and this is further integrated to determine the angular position. All calculations are performed by separating the space variables into their real and imaginary components, utilizing auxiliary variables to simplify the model's calculations.

Regarding the simulation, it is observed that the original model, based on the fundamental harmonic, exhibits completely clean signals, without distortions or impacts on variables such as stator currents, angular speed, and electrical torque. However, when incorporating space harmonics, their impact becomes evident in various variables and in the operational characteristics of the electromechanical converter.

Therefore, it is crucial to consider the influence of space harmonics in the analysis of the induction machine, as they can negatively affect its performance, efficiency, and lifespan. These harmonics generate fluctuations in electrical torque, angular speed, and stator currents, introducing vibrations, noise, and electromagnetic interferences. Finally, including the presence of space harmonics in the design of the induction machine allows for a more realistic approximation of its behavior and the industrial needs that arise in practice.

5. CONCLUSION

In this work, an original model of the induction machine has been developed that integrates space harmonics, space vectors in stator-rotor coordinates, and the VBR technique, which has been successfully implemented in the ATP-EMTP tool through its graphical environment ATPDraw. It has been demonstrated that space harmonics, particularly the fifth and seventh harmonics, significantly impact the operation of induction machines. Simulations conducted with ATP-EMTP have shown fluctuations in current and torque, negatively affecting the efficiency and operability of these machines. The results obtained emphasize the importance of considering harmonic effects when designing and operating these machines in industrial environments.

This work provides a more detailed understanding of the impact of space harmonics on the performance of induction machines, which is crucial for enhancing operability and efficiency in industrial applications. This research contributes to improving the analysis of induction machines, facilitating more efficient operation in the presence of space harmonic distortions.

FUNDING INFORMATION

Authors state no funding involved.

AUTHOR CONTRIBUTIONS STATEMENT

This journal uses the Contributor Roles Taxonomy (CRediT) to recognize individual author contributions, reduce authorship disputes, and facilitate collaboration.

Name of Author	C	M	So	Va	Fo	I	R	D	O	E	Vi	Su	P	Fu
Jose Manuel Aller	✓	✓	✓	✓	✓	✓		✓	✓	✓		✓	✓	✓
Ruben Nicolas Guevara		✓	✓	✓		✓		✓	✓	✓	✓			
Bryam Steven Pulla		✓	✓	✓		✓		✓	✓	✓	✓			

C : **C**onceptualization
M : **M**ethodology
So : **So**ftware
Va : **Va**lidation
Fo : **Fo**rmal analysis
I : **I**nvestigation
R : **R**esources
D : **D**ata Curation
O : Writing - **O**riginal Draft
E : Writing - Review & **E**diting
Vi : **Vi**sualization
Su : **Su**pervision
P : **P**roject administration
Fu : **Fu**nding acquisition

CONFLICT OF INTEREST STATEMENT

Authors state no conflict of interest.

DATA AVAILABILITY

The authors confirm that the data supporting the findings of this study (ATPDraw model and models code) in Figures 13 and 14. Additionally, derived data supporting these findings can be obtained from the corresponding author [JMA] upon request at the email address: jaller@ups.edu.ec.

REFERENCES

[1] C. Huang, S. Bu, H. H. Lee, K. W. Chan, and W. K. C. Yung, "Prognostics and health management for induction machines: a comprehensive review," *Journal of Intelligent Manufacturing*, vol. 35, no. 3, p. 937 – 962, 2024, doi: 10.1007/s10845-023-02103-6.

[2] G. Grewal, B. Rajpurohit, and J. Singh, "Energy management in steel rolling plant," *in Proceedings of the 2014 International Conference and Utility Exhibition on Green Energy for Sustainable Development*, ICUE 2014, pp. 1-7, 2014.

[3] N. Tesla, "Electro—magnetic motor," 1891, u.S. Patent 445,207, May 20, 1889, January 27, 1891.

[4] G. Ferraris, "Experiments on the rotatory magnetic field," *Atti della Reale Accademia delle Scienze di Torino*, vol. 23, pp. 849–863, 1888.

[5] F. Giannini and M. Savio, "Galileo ferraris and the origins of the induction motor," *IEEE Industry Applications Magazine*, vol. 14, no. 2, pp. 52–61, 2008, doi: 10.1109/ISEMC.2005.1614494.

[6] M. von Dolivo-Dobrovolsky, "Alternating-current motor," 1890, u.S. Patent 427,978, May 13, 1890.

[7] G. Ferraris and R. Arno, "Arrangement for starting alternating-current motors." 1899, u.S. Patent 629,897, August 1, 1899.

[8] N. S. Khumalo, N. P. Memane, and U. B. Akuru, "Performance and safety improvement of induction motors based on testing and evaluation standards," *CES Transactions on Electrical Machines and Systems*, vol. 8, no. 3, p. 310 – 318, 2024, doi: 10.30941/CESTEMS.2024.00018.

[9] K. L. Hansen, "Torque components due to space harmonics in induction motors," *Journal of the American Institute of Electrical Engineers*, vol. 41, no. 12, pp. 928–932, 1922, doi: 10.1109/JoAIEE.1922.6593215.

[10] C. A. M. Weber and F. W. Lee, "Harmonics due to slot openings," *Transactions of the American Institute of Electrical Engineers*, vol. XLIII, pp. 687–694, 1924, doi: 10.1109/T-AIEE.1924.5061020.

[11] B. Brkovic and M. Jecmenica, "Calculation of rotor harmonic losses in multiphase induction machines," *Machines*, vol. 10, no. 5, 2022, doi: 10.3390/machines10050401.

[12] L. Schreier, J. Bendl, and M. Chomat, "Analysis of influence of third spatial harmonic on currents and torque of multi-phase synchronous machine with permanent magnets," *Electrical Engineering*, vol. 100, no. 3, p. 2095–2102, 2018, doi: 10.1007/s00202-018-0686-8.

[13] H. Gorginpour, H. Oraee, and R. A. McMahon, "Electromagnetic-thermal design optimization of the brushless doubly fed induction generator," *IEEE Transactions on Industrial Electronics*, vol. 61, no. 4, p. 1710 – 1721, 2014, doi: 10.1109/TIE.2013.2267705.

[14] K. Hurst, T. Habetler, G. Griva, and F. Profumo, "Sensorless speed measurement using current harmonic spectral estimation in induction machine drives," *Industry Applications, IEEE Transactions on*, vol. 30, no. 4, pp. 865–873, 1994, doi: 10.1109/63.484418.

[15] D. Stincescu and P. Viarouge, "A general approach of space and time harmonics interactions in induction motors," *Electromagnetic Compatibility*, 2005. EMC 2005. International Symposium on, pp. 72–77, 2005, doi: 10.1109/ISEMC.2005.1614494.

[16] G. Retter, Matrix and Space Vector Theory of Electrical Machines. Budapest: Akademia Kiado, 1987.

[17] J. W. Rengifo-Santana, J. Benzaquen-Su˜ne, J. M. Aller-Castro, A. A. Bueno-Montilla, and J. A. Restrepo-Zambrano, "Parameter estimation method for induction machines using instantaneous voltage and current measurements," *Revista Facultad de Ingenieria*, vol. 1, no. 75, p. 57 – 66, 2015, doi: 10.17533/udea.redin.n75a07.

[18] L. Wang, J. Jatskevich, and S. D. Pekarek, "Modeling of induction machines using a voltage-behind-reactance formulation," *IEEE Transactions on Energy Conversion*, vol. 23, no. 2, pp. 382–392, 2008, doi: 10.1109/TEC.2008.918601.

[19] L. Wang and J. Jatskevich, "Approximate voltage-behind-reactance induction machine model for efficient interface with emtp network solution," *IEEE Transactions on Power Systems*, vol. 25, no. 2, p. 1016 – 1031, 2010, doi: 10.1109/TPWRS.2009.2034526.

[20] N. Amiri, S. Ebrahimi, and J. Jatskevich, "Saturable voltage-behind-reactance models of induction machines including air-gap flux harmonics," *IEEE Transactions on Energy Conversion*, vol. 38, no. 3, p. 2022 – 2033, 2023, doi: 10.1109/TEC.2023.3259385.

[21] A. M. Orellana, C. D. Rodriguez, L. J. Orozco, W. P. Correa, and J. M. Aller, "Field-oriented control of an induction machine using ATPDraw and MODELS," *in ECTM 2023 - 2023 IEEE 7th Ecuador Technical Chapters Meeting,* 2023, doi: 10.1109/ETCM58927.2023.10308999.

[22] M. Wieczorek and E. Rosolowski, "Modelling of induction motor for simulation of internal faults," *in Proceedings - International Symposium: Modern Electric Power Systems, MEPS'10*, 2010, pp. 1-6.

[23] L. W. Buchanan, "An equivalent circuit for a single-phase motor having space harmonics in its magnetic field," *IEEE Transactions on Power Apparatus and Systems*, vol. 84, no. 11, pp. 999–1007, 1965, doi: 10.1109/TPAS.1965.4766130.

[24] Y. Anazawa, A. Kaga, H. Akagami, S. Watabe, and M. Makino, "Prevention of harmonic torques in squirrel cage induction motors by means of soft ferrite magnetic wedges," IEEE Transactions on Magnetics, vol. 18, no. 6, pp. 1550–1552, 1982, doi: 10.1109/TMAG.1982.1062116.

[25] C. F. Landt, "A technique for assessing space harmonic effects in squirrel cage induction motors," *Transactions of the South African Institute of Electrical Engineers*, vol. 73, no. 1, pp. 2–9, 1982.

[26] S. Tanneeru, J. Mitra, Y. J. Patil, and S. J. Ranade, "Effect of large induction motors on the transient stability of power systems," *in 2007 39th North American Power Symposium, NAPS*, 2007, pp. 223–228, doi: 10.1109/NAPS.2007.4402314.

[27] B. Nomikos, E. Potamianakis, and C. Vournas, "Oscillatory stability and limit cycle in an autonomous system with wind generation," *in 2005 IEEE Russia Power Tech PowerTech*, 2005, doi: 10.1109/PTC.2005.4524830.

[28] M. Cerrada, D. Jim´enez-Sant´ın, R. Ortega, J. M. Aller, D. Cabrera, and R.-V. S´anchez, "A simple yet realistic integrated dynamical modeling of an induction motor and one-stage spur gearbox system with broken tooth," *Mechanism and Machine Theory*, vol. 200, 2024, doi: 10.1016/j.mechmachtheory.2024.105694.

[29] B. S. Pulla and R. N. Guevara, "Modeling and validation of the dynamic behavior of induction machines in ATP-EMTP with spatial harmonics in ATPDraw (in Spanish)," *Direcci´on de Electricidad' Tech. Rep.*, Feb 2025.

BIOGRAPHIES OF AUTHORS

José Manuel Aller was born in Caracas, Venezuela, in 1958. He received the B.Sc. degree in electrical engineering from the Universidad Simón Bolívar, Caracas, in 1980, the M.S. degree in electrical engineering from the Universidad Central de Venezuela, Caracas, in 1982, and the Ph.D. degree in Industrial Engineering from the Universidad Politécnica de Madrid, Spain, in 1993. Dr. Aller has been a lecturer at the Universidad Simón Bolívar for 36 years. From 2001 to 2005, he served as the General Secretary of the Universidad Simón Bolívar. He was also a Visiting Professor at the Georgia Institute of Technology, Atlanta, GA, USA, in 2000 and 2007. Since 2016, he has been a Full-Time Professor of electrical machines and electromagnetism in the Department of Electrical Engineering at the Universidad Politécnica Salesiana, Cuenca, Ecuador. Dr. Aller has published over 120 papers in his field. His research interests include space-vector applications, electrical machine control, power electronics, and the monitoring of electrical machines. He can be contacted at email: jaller@ups.edu.ec.

Ruben Nicolas Guevara born in Cuenca, Ecuador, in 2001, he studied at Alborada School in Cuenca, where he earned his Bachelor's degree in science. In 2025, he graduated as an electrical engineer from the Salesian Polytechnic University, which is internationally accredited by ABET. He completed his professional internship at the Mobility Company of Cuenca, which manages, administers, and maintains the Cuenca Tram in Ecuador, where he gained valuable knowledge in electrical infrastructure and transportation system maintenance. In 2024, he carried out his final degree project in the area of space harmonics in induction machines, acquiring academic and professional experience in the modeling and analysis of this type of electromechanical converter. His interests focus on the study of electric machines, power electronics, and alternative energies. He can be contacted at: rguevarav1@est.ups.edu.ec.

Bryam Steven Pulla born in Cuenca, Ecuador, in 2002, he graduated with a Bachelor's degree in Science from the Millennium Educational Unit Francisco Febres Cordero in Cuenca. In 2025, he earned his degree in electrical engineering from the Salesian Polytechnic University, which is internationally accredited by ABET. He completed his professional internship at the Electric Company (INDEC) Consortium PMC, where he gained practical experience in the design of electrical distribution networks, surveying existing distribution networks, and the redesign and adaptation of distribution systems for the electric company CENTROSUR, including data registration and management in the system. In 2024, he conducted his final degree project in the area of space harmonics in induction machines, acquiring both academic and professional experience in the modeling and analysis of this type of electromechanical converter. His interests focus on the design and operation of electrical protections, the study of electric machines, distribution systems, and alternative energies. He can be contacted at: bpullap@est.ups.edu.ec.